Published in final edited form as:
Biotechniques. ; 56(5): 239–249. doi:10.2144/000114166.

Isolation and characterization of mammalian cells expressing the *Arf* promoter during eye development

Nida S. Iqbal[1,3], **Lin Xu**[1,3], **Caitlin C. Devitt**[1], and **Stephen X. Skapek**[1,2,4]

[1]Department of Pediatrics, Division of Hematology/Oncology, University of Texas Southwestern Medical Center, Dallas, TX

[2]Center for Cancer and Blood Disorders, Children's Medical Center, Dallas, TX

Abstract

Although many researchers have successfully uncovered novel functions of the tumor suppressor $p19^{Arf}$ utilizing various types of cultured cancer cells and immortalized fibroblasts, these systems do not accurately reflect the endogenous environment in which *Arf* is developmentally expressed. We addressed this by isolating perivascular cells from the primary vitreous of the mouse eye. These cells represent a rare cell type that normally expresses the $p19^{Arf}$ tumor suppressor in a non-pathological, developmental context. We utilized fluorescence activated cell sorting to purify the cells by virtue of a GFP reporter driven by the native *Arf* promoter, and characterized their morphology and gene expression pattern. We further examined the effects of reintroduction of *Arf* in the PVCs to verify expected downstream effectors of $p19^{Arf}$ as well as uncover novel functions as a regulator of vasculogenesis. This methodology and cell culture model should serve as a useful tool to examine $p19^{Arf}$ biology.

Keywords

$p19^{Arf}$; primary vitreous; perivascular cells; primary cell isolation; Arf; eye development; hyaloid regression

Introduction

Over the last two decades, our understanding of the regulation of the tumor suppressor, $p19^{Arf}$, has grown, as has our understanding of its tumor suppression, primarily by controlling p53. The original model supported the notion that $p19^{Arf}$ induction antagonizes Mdm2, the negative regulator of p53; the stabilized p53 promotes the progression of a transcriptional program that, ultimately, arrests cell proliferation, facilitates DNA damage

[4]Corresponding author: Stephen X. Skapek, MD, Department of Pediatrics, Division of Hematology/Oncology, Mail Code 9063, University of Texas Southwestern Medical Center, 5323 Harry Hines Blvd, Mail Code 9063, Dallas TX 75390. Telephone: 214-648-3081, Fax: 214-648-3122, Stephen.skapek@utsouthwestern.edu.
[3]These authors contributed equally to the manuscript

Author Contributions: NSI and CCD performed mouse embryo dissections and specimen collections. NSI maintained the cells, prepared material for RNA-seq and performed functional experiments. LX performed all the data analysis for RNA-seq. SXS guided the overall direction of the research project, helped to analyze and interpret data, and helped to write final versions of the manuscript. All authors made substantial contributions to writing the manuscript.

Competing Interests Statement: The authors declare no competing interests.

responses, or promotes apoptosis (1-4). Ample evidence indicates that $p19^{Arf}$ also acts independently of p53. This was first suggested by the differences in the types and latency of spontaneous tumors in animals lacking either *p53* or *Arf* and in mice lacking both (5,6). Established p53-independent functions of $p19^{Arf}$ include regulation of rRNA biogenesis via its interaction with NPM/B23 (7,8); inhibition of transactivation by c-Myc (9,10) and E2F1 (11); sumoylation of Mdm2, NPM and others (12,13); as well as inhibition of $NF_{\kappa}B$ (14). While these studies have been vital for ascribing functions to the tumor suppressor, their significance is sometimes subject to question because the work was not accomplished in cells that normally express *Arf*. Indeed, one of the clearest *in vivo* examples of a p53-independent role for $p19^{Arf}$ resides in its capacity to block Pdgfrβ expression and proliferation of perivascular cells of the developing eye to foster involution of the underlying hyaloid vessels (15-18).

Despite wide-spread importance of perivascular cells to support vascular integrity, robust *Arf* expression is only observed in the perivascular cells flanking the hyaloid vessels and the internal umbilical artery (19), both of which represent vascular beds that are not necessary beyond embryo development. In the absence of $p19^{Arf}$, Pdgfrβ accumulates in the perivascular cells and leads to hyperplasia of cells in the vitreous space. This results in a retrolental mass and causes catastrophic secondary effects on the lens and retina, leaving the animals blind (17,20). Even though it is clear that the developmental function of $p19^{Arf}$ is imperative to the animal, little is known about the particular perivascular cells that normally express the tumor suppressor gene.

In order to better understand $p19^{Arf}$ function during development, we isolated cells that normally activate the *Arf* promoter from the vitreous compartment of the eye. We were able to purify cells endogenously expressing the *Arf* promoter by fluorescence activated cell sorting (FACS) and examine them in culture. In this report, we describe the isolation and *in vitro* culture of *Arf* expressing primary vitreous cells (PVCs) and compare them to previously established cell culture models for studying *Arf* function. By global transcriptome analysis, we gain clearer insight into the identity of the PVCs and further demonstrate the utility of these cells by examining expected and novel molecular changes upon reintroduction of *Arf*. The availability and use of the $Arf^{GFP/GFP}$ PVCs holds great potential for better understanding the role of $p19^{Arf}$ in mammalian development and how these functions are abrogated in human ocular and cardiovascular disease as well as tumorigenesis.

Materials and Methods

Animals

Mice in which *Arf* exon 1β is replaced by a reporter gene encoding green fluorescence protein (GFP) (21) were maintained in a mixed C57BL/6 × 129/Sv genetic background. Primary MEFs from $Arf^{lacZ/lacZ}$ mice were derived as previously described (17). Animal studies were accomplished at the University of Texas Southwestern Medical Center, with approval of the animal care and use committees.

Eyes were isolated from $Arf^{GFP/GFP}$ mice, euthanized and decapitated at postnatal days (P) 0 - 4. The eyelid was incised using a No. 11, straight surgical blade (Feather Safety Razor Co.) to expose the eye. While holding the eyelid open, the scalpel blade was used to transect extra-ocular muscles and other connective tissue between the globe and the bony orbit. Small angled forceps (Fine Science Tools) were inserted between the orbit and globe, grasping the optic nerve/ophthalmic vessels firmly and gently lifting out the intact eye. Enucleated eyes were submerged in ice-cold PBS and stabilized under PBS by holding the optic nerve stub. Small spring scissors (Fine Science Tools) were used to cut along the circumference of the eye at the equator. The cornea/anterior part of the sclera were lifted off, leaving the optic cup and lens together under PBS. The retina was then removed in piecemeal fashion, leaving the lens with attached retrolental mass.

Cell Isolation and Culture

The lens/retrolental mass tissue from 60 individual eyes were pooled in a 1.5 mL microcentrifuge tube and digested in M2 media with 300 μg/mL hyaluronidase and 1 mg/mL collagenase (all from Sigma-Aldrich) at 37° C for 15 minutes. The tissue was briefly triturated and further incubated at 37° C for 10 minutes. Digested material (including undigested lenses) was centrifuged, washed with D-MEM with 20% FBS, and then resuspended in D-MEM/20% FBS with penicillin/streptomycin. Resuspended cells (including PVCs) were passed through a 35 μM filter into polystyrene tube for FACS. GFP-positive PVCs were collected using the MoFlo (Dakocytomation) cell sorter. Sorted PVCs were plated (6,000 cells/well) in a 96-well plate with Pericyte Medium (PM) (ScienCell). Cells were passed (1:4) using trypsin/EDTA every 3 days.

$Arf^{lacZ/lacZ}$ MEFs (19), 10T1/2 fibroblasts and PVCs were used for RNA-Seq analysis. Briefly, cells were plated at a density of 1×10^6 cells/ 10 cm plate and cultivated in PM until ~80% confluence, at which point cells were harvested for RNA extraction.

Whole Transcriptome Sequencing (RNA-Seq)

Total RNA was isolated using the miRNeasy mini kit (Qiagen) and treated with RNase free DNaseI to remove genomic DNA (Qiagen). RNA integrity and purity was determined using the Bioanalyser Pico Chip (Agilent), assuring that each sample had a RIN score of 10. RNA (1 μg) from two biological replicates of each cell type was fragmented in the UT Southwestern Next-Generation Sequencing core, converted to cDNA, and amplified by PCR according to the Illumina RNA-Seq protocol (Illumina, Inc. San Diego, CA). The Illumina HiSeq 2000 (San Diego, CA) instrument was used to generate 50 bp single-end sequence reads. RNA-Seq read quality was evaluated in the core using the Illumina purity filter and distribution of base quality scores at each cycle.

Sequence reads for each sample were aligned to the UCSC mm10 version of the mouse reference genome assembly using Bowtie 2.1.0 (22) and the splicing-aware aligner TopHat 2.0.8 (23). The alignment allows only uniquely aligned reads and up to two mismatches per read. All other parameters were set to the default values. The quality of the RNA-Seq data was evaluated by FastQC (v0.10.1) and a series of Perl (v5.16.1) and R (v3.0.1) scripts. Normalized gene expression values expressed as fragments per kilobase of exon per million

fragments mapped (FPKM) were determined using Cufflinks 2.0.2 (24) with default settings, which reports the mean of the maximum likelihood estimates from each of three replicates processed independently.

Western blotting

Protein expression was examined by Western-blotting according to a standard procedure. The following antibodies were used: anti-$p19^{Arf}$ (Ab80, Abcam, 1:1000), anti-p21 (Sc-756, Santa Cruz, 1:1000), anti-p53 (Sc-6243, Santa Cruz, 1:1000), anti-MDM2 (Sc-965, Santa Cruz 1:1000) and anti-Hsc70 (Sc-1059, Santa Cruz, 1:5,000).

Quantitative RT-PCR (qRT-PCR)

Total RNA was extracted from PVCs using the miRNeasy mini kit (Qiagen). For qRT-PCR, 1 μg of total RNA was reverse transcribed using *NCode miRNA* First-Strand Synthesis (Invitrogen) and KAPA SYBR Green Master Mix (KAPA). qRT-PCR was performed in a 96-well plate using BioRad instrument. The PCR program consisted of 20 sec at 95 C, followed by 40 cycles of 95 C for 15s and 60 C for 20s. Primer quality was analyzed by dissociation curves. The expression of mir34abc and *Pdgfrα, Pdgfrβ and αSMA* was normalized to *U6* and *Gapdh*, respectively.

Results and Discussion

Currently, there is very little known about the cells that normally express *Arf*, motivating us to generate a cell culture model that accurately reflects the unique environment in which *Arf* is expressed developmentally. We decided to pursue this by taking advantage of $Arf^{GFP/GFP}$ mice in which GFP replaces exon 1β of the endogenous *Arf* locus, rendering the mice *Arf* null. In this context, a retrolental mass persists in the primary vitreous space in which GFP (+), *Arf*-expressing cells, in addition to other cell types including endothelial cells, are present (Figure 1A). It is important to note that the retrolental mass is not evident in WT or GFP/+ animals postnatally, making it unfeasible to derive these cells under “wild type” conditions. We isolated the retrolental tissue from $Arf^{GFP/GFP}$ mice and retrieved a total of 38,000 GFP-positive cells (averaging 633 cells/eye), which represented 2-3% of the total population (Figure 1B). We collected the $Arf^{GFP/GFP}$ Primary Vitreous Cells (PVCs) for *in vitro* culture and expansion. At confluence, the PVCs form a monolayer and adopt a fibroblast-like morphology with some variation in GFP expression (Figure 1C). We continued to expand the cells in culture and observed that GFP expression persists through passage 15 (data not shown). At passage 5 and sub-confluence, the PVCs are elongated and spindle-like with long cytoplasmic processes. The cells continue to express GFP while WT MEF cells cultured in tandem do not (Figure 1D). Although many laboratories, including our own, have successfully utilized classically immortalized fibroblasts and cancer cell models to gain valuable insight into some of the developmental and tumor suppressive functions of *Arf*, these systems are imperfect in recapitulating the non-pathological environment in which *Arf* is expressed. The PVCs represent, for the first time, a cell culture model in which the *Arf* promoter is endogenously turned on during development allowing us and other researchers to explore the capacity of $p19^{Arf}$ to control vascular remodeling and

mural cell proliferation in the context of a cell that normally expresses this promoter. These cells will also be useful in clarifying the complex regulation of the *Arf* promoter.

Because we have not unequivocally established the identity of the *Arf*-expressing cells, we sought to capture the global gene expression profile of the $Arf^{GFP/GFP}$ PVCs in comparison to other cell culture models that have been previously used to study *Arf* biology. Like the PVCs, $Arf^{lacZ/lacZ}$ MEFs do not express a functional $p19^{Arf}$ protein, while 10T1/2 cells, a widely used pericyte model, carry a biallelic deletion of *Arf* (19,21)*(and unpublished data)*. When cultured in Pericyte Medium, all three cell lines resemble fibroblasts in their morphology (Figure 2A). To define these cells by gene expression, we cultured the $Arf^{GFP/GFP}$ PVCs, $Arf^{lacZ/lacZ}$ MEFs and 10T1/2 cells, extracted total RNA and performed high-throughput RNA-sequencing. We observed 85.3, 86.7 and 83.8 million sequence reads for $Arf^{lacZ/lacZ}$ MEFs, 10T1/2 and PVCs, respectively; after applying a series of computational tools (see Methods), we were left with 71.6, 81.9 and 73.5 million reads that were successfully mapped to the mouse reference genome. We examined how all 10,704 genes expressed in PVCs partitioned between $Arf^{lacZ/lacZ}$ MEFs and 10T1/2 cells. We found 970 expressed genes in PVCs that were also expressed in either $Arf^{lacZ/lacZ}$ MEFs or 10T1/2 cells; 769 genes were expressed in $Arf^{lacZ/lacZ}$ MEFs, while 201 were found in 10T1/2 cells (binomial test, $P = 2.8\times10^{-79}$) (Figure 2B). Based on this analysis, we conclude that on a genome-wide scale, the $Arf^{GFP/GFP}$ PVC*s* are more closely related to the $Arf^{lacZ/lacZ}$ MEFs than the 10T1/2 cells.

The fact that the MEFs and the PVCs share 86% similarity in gene expression reaffirmed our previous studies utilizing $Arf^{lacZ/lacZ}$ MEFs to establish a pathway beginning from *Arf* induction to characterization of its downstream effects required for eye development. We have previously established that Tgfβ signaling drives *Arf* expression in $Arf^{lacZ/lacZ}$ MEFS and *in vivo* resulting in $p19^{Arf}$ mediated down-regulation of Pdgfrβ (19,25). In order to understand if the $Arf^{GFP/GFP}$ PVCs were similar to the $Arf^{lacZ/lacZ}$ MEFs in this regard, we looked for the expression of all Tgf-beta pathway genes as defined by KEGG and performed a hierarchical clustering (26,27). We found the components of the Tgfβ pathway that we have so far defined as important for *Arf* regulation, including *Smad2/3*, *Sp1* and *Cebpβ* to be expressed in all three cell lines (Figure 2B) (28). Further, based on all Tgfβ pathway genes, we found that the PVCs clustered more closely to the $Arf^{lacZ/lacZ}$ MEFs than the 10T1/2 cells (supplemental).

To explicitly establish our previous finding that the *Arf*-expressing cells of the primary vitreous are perivascular, we examined the expression of known markers that identify vascular/mural cells, as well as fibroblasts, endothelial cells and retinal cells. As we have previously shown, the $Arf^{GFP/GFP}$ PVCs express the transmembrane cell surface protein *Pdgfrβ* (17,18,29). We also observed expression of, *Angpt1*, which is critical for angiogenesis and vessel maturation as well as *α-SMA*, a bona fide perivascular cell marker (30). *Vimentin*, a cytoskeletal component associated with mesenchymal cells, was also highly expressed in all three cell lines, further establishing that these cells are perivascular (Figure 2D) (31). We found several markers of fibroblasts such as *S100a4, Col1a1 and Ph4b* to be expressed in all three cell types, while *Fap*, a marker of differentiated fibroblasts, was only present in the $Arf^{lacZ/lacZ}$ MEFs (Figure 2D) (32). Further, we observed the lack of

expression of endothelial specific genes, *Pecam, Cdh5 and vWf*, demonstrating that *Arf* is not expressed in the endothelial cell population that coexists with the PVCs in the developing eye (Figure 2D) (33). Finally, to ensure that we did not contaminate our cell prep with neighboring retinal tissue, we checked for the expression of known retinal defining transcription factors: *Six3, Otx2, Nr2e3, Nrl* and *Crx* (34). None of these transcription factors were expressed in either cell line (Figure 2D). Based on this gene expression signature and the morphology of the cells, we assert that our $Arf^{GFP/GFP}$ PVCs are perivascular cells.

While we observed that 86% of all the genes expressed in the $Arf^{GFP/GFP}$ PVCs were also expressed in the $Arf^{lacZ/lacZ}$ MEFs, we found 323 genes representing 3% of the total genes expressed in PVCs to be mutually exclusive from those genes expressed in MEFs and 10T1/2 cells (Figure 2B). To understand how the PVCs are distinct from the other cultured cells, we subjected the dissimilar set of genes to Gene Ontology (GO) pathway analysis. KEGG pathway and GO terms were collected from the Molecular Signatures Database (35). We highlighted several pathways that were enriched in the $Arf^{GFP/GFP}$ PVCs ($p > 0.05$) (Figure 3A, extensive list supplemental). Given their neural crest origin, it was not unexpected that we observed that the PVC only genes were enriched for the term Nervous System Development (25). Of interest, we found that the term Anatomical Structure Morphogenesis was enriched with 9 genes expressed in the $Arf^{GFP/GFP}$ PVCs (-log p value = 2.84) including Pax6 and Eya2, both of which are important for eye development (Figure 3A) (36). Only the $Arf^{GFP/GFP}$ PVCs were significantly enriched for genes in the Tgfβ Receptor Signaling Pathway, including *Gdf15, Eng and Lefty1;* perhaps suggesting that the PVCs more aptly reflect a signaling environment to endogenously regulate *Arf* (Figure 3A and supplemental). We also found the terms Cell Proliferation, Cellular Localization and Cell-cell Signaling to be enriched in the PVC only gene set, reflecting the dynamic environment of the vitreous compartment as well as the requirement of $p19^{Arf}$ to blunt the proliferation of these cells.

We recently identified a previously unrecognized role for $p19^{Arf}$ during development in its capacity to regulate microRNA expression independently of p53 (37). With this in mind, we sought to understand functional pathways targeted by microRNAs expressed in the PVCs. We found of all 10,704 genes expressed, 1.8% or 186 represented small non-coding RNA genes, 80 of which are defined as microRNAs based on annotation mm10 from the UCSC Genome Browser (data not shown)(38). In order to understand the function of the microRNAs, we analyzed all microRNAS expressed in the $Arf^{GFP/GFP}$ PVCs by DIANA-miRPath v2.0, a web-based server for microRNA target prediction and pathway analysis (39). The most significantly enriched pathway targeted by microRNAs expressed in the $Arf^{GFP/GFP}$ PVCs was ECM-receptor interaction with 10 microRNAs expressed that target 21 different genes in this pathway (-log p value = 13.8) (Figure 3B). Of interest, Tgf-beta signaling was also enriched in both the $Arf^{GFP/GFP}$ PVCs and $Arf^{lacZ/lacZ}$ MEFs (Figure 3B and data not shown). The $Arf^{GFP/GFP}$ PVCs expressed 12 microRNAs targeting 38 genes within this pathway (-log p value = 1.48) (Figure 3B). Tgf-beta regulated microRNAs are known to target genes that promote angiogenesis and components of the epithelial to mesenchymal transition (EMT) program (40). In this regard, we also found the terms Focal

adhesion, Pathways in cancer and Transcriptional misregulation in cancer to have significant enrichment of genes targeted by the repertoire of microRNAs expressed in the PVCs.

In line with the idea that these cells are derived from the neural crest, evidenced by lineage-tracing experiments using *Wnt1-Cre, Rosa26-LSL-tdTomato* and *Wnt1-Cre, Arf*$^{fl/fl}$ mouse models, and thus have undergone EMT, we were prompted to examine the expression of EMT associated genes in the PVCs (Figure 3C) (25). We found high expression of known mesenchymal marker genes (*Cdh2)* as well as transcription factors such as *Twist1, Zeb1/2 and Snai1* that are required for EMT (40). In contrast, the classical epithelial marker *Cdh1 (E-cadherin)*, was not expressed. Because p19^{Arf} is turned on after the cells have migrated, an intriguing hypothesis posits that p19^{Arf} expression in these cells negatively regulates the EMT program by inhibiting their proliferation and migration. Our *in vitro* model of the *Arf*$^{GFP/GFP}$ PVCs will be ideal for investigating how p19^{Arf} controls aspects of the EMT program.

While characterizing these cells is critical, the real utility in this model stems from wanting to understand *Arf* activity in a cell that normally expresses the gene during development. To address this, we ectopically expressed *Arf-RFP* by retroviral transduction in the *Arf*$^{GFP/GFP}$ PVCs (Figure 4A). Upon ectopic *Arf* expression, we observed activation of the p53 pathway as detected by expression of downstream target effectors that have been previously described, p53, MDM2 and p21 as compared to the RFP control (Figure 4A) (3). Moreover, we have recently showed that the expression of the miR-34 family is dependent upon *Arf* status in cultured cells and *in vivo*. In our analysis, we observed that ectopic *Arf* expression could upregulate all three members of the miR-34 family, miR-34abc in MEFs triple negative for *p53*, *MDM2* and *Arf* (TKO MEFs). Furthermore, shRNA knockdown of p19^{Arf} in *p53-/- MEFs*, reduced the expression of miR-34abc (37). In the *Arf*$^{GFP/GFP}$ PVCs, we observed that ectopic *Arf* expression induced miR-34a and decreased the expression of miR-34b. miR-34c was not affected by p19^{Arf} in these cells (Figure 4C). Finally, because we observed that the PVCs had undergone EMT and expressed mesenchymal genes, we became interested in how re-expression of Arf affected vascular gene expression. As we have shown previously, Pdgfrβ is down-regulated in response to overexpression of *Arf* (17,18). Pdgfr*a* mRNA was not affected by *Arf*, while *αSMA* was significantly decreased upon reintroduction of *Arf* suggesting that it may play a role in regulating vascular gene expression. These cells will be a useful tool in clarifying how p19^{Arf} affects vascular smooth muscle biology.

We believe that the PVCs will represent an important model for studying *Arf*, particularly for studies focused on how the *Arf* promoter is activated and the functional consequence of p19^{Arf} expression in these cells. Furthermore, heterotypic interactions between perivascular and endothelial cells help to drive vascular stabilization and remodeling. Indeed, the molecular mechanism by which p19^{Arf} regulates vascular/mural cell identity and proliferation, as well as the contribution of the human *CDKN2A* locus and intergenic 9p21 region to cardiovascular disease risk remain unclear. In our model, loss of *Arf* in perivascular cells seems to derail the developmentally-timed regression of the underlying endothelial cells of the hyaloid vasculature. Given that *Arf* expression in normal cells is largely limited to perivascular cells embracing two vascular structures that become

essentially functionless in the postnatal period, these cells could be particularly valuable tools to study perivascular-endothelial cell interactions. Additionally, by examining microRNA and protein changes that occur when *Arf* is expressed in these cells, we will be able to better understand the full repertoire of $p19^{Arf}$ dependent changes that drive vascular involution.

Supplementary Material

Refer to Web version on PubMed Central for supplementary material.

Acknowledgments

We gratefully acknowledge C. J. Sherr (St. Jude Children's Research Hospital) for providing $Arf^{GFP/GFP}$ mice; Flow Cytometry Core Facility at UT Southwestern Medical Center and the UT Southwestern McDermott DNA Sequencing Core for next generation sequencing support. This research is supported by grants to SXS from the National Eye Institute (EY 014368 and EY 019942).

References

1. Kamijo T, Weber JD, Zambetti G, Zindy F, Roussel MF, Sherr CJ. Functional and physical interactions of the ARF tumor suppressor with p53 and Mdm2. Proc Natl Acad Sci USA. 1998; 95:8292–8297. [PubMed: 9653180]
2. Pomerantz J, Schreiber-Agus N, Liegeois NJ, Silverman A, Alland L, Chin L, Potes J, Chen K, et al. The Ink4a tumor suppressor gene product, p19Arf, interacts with MDM2 and neutralizes MDM2's inhibition of p53. Cell. 1998; 92:713–723. [PubMed: 9529248]
3. Zhang Y, Xiong Y, Yarbrough WG. ARF Promotes MDM2 Degradation and Stabilizes p53: ARF-INK4a Locus Deletion Impairs Both the Rb and p53 Tumor Suppression Pathways. Cell. 1998; 92:725–734. [PubMed: 9529249]
4. Ko LJ, Prives C. p53: puzzle and paradigm. Genes & development. 1996; 10:1054–1072. [PubMed: 8654922]
5. Jacks T, Remington L, Williams BO, Schmitt EM, Halachmi S, Bronson RT, Weinberg RA. Tumor spectrum analysis in p53-mutant mice. Current biology : CB. 1994; 4:1–7. [PubMed: 7922305]
6. Kamijo T, Bodner S, van de Kamp E, Randle DH, Sherr CJ. Tumor spectrum in ARF-deficient mice. Cancer research. 1999; 59:2217–2222. [PubMed: 10232611]
7. Itahana K, Bhat KP, Jin A, Itahana Y, Hawke D, Kobayashi R, Zhang Y. Tumor suppressor ARF degrades B23, a nucleolar protein involved in ribosome biogenesis and cell proliferation. Molecular cell. 2003; 12:1151–1164. [PubMed: 14636574]
8. Sugimoto M, Kuo ML, Roussel MF, Sherr CJ. Nucleolar Arf tumor suppressor inhibits ribosomal RNA processing. Molecular cell. 2003; 11:415–424. [PubMed: 12620229]
9. Datta A, Nag A, Pan W, Hay N, Gartel AL, Colamonici O, Mori Y, Raychaudhuri P. Myc-ARF (alternate reading frame) interaction inhibits the functions of Myc. J Biol Chem. 2004; 279:36698–36707. [PubMed: 15199070]
10. Qi Y, Gregory MA, Li Z, Brousal JP, West K, Hann SR. p19Arf directly and differentially controls the functions of c-Myc independently of p53. Nature. 2004; 431:712–717. [PubMed: 15361884]
11. Eymin B, Karayan L, Seite P, Brambilla C, Brambilla E, Larsen CJ, Gazzeri S. Human ARF binds E2F1 and inhibits its transcriptional activity. Oncogene. 2001; 20:1033–1041. [PubMed: 11314038]
12. Rizos H, Woodruff S, Kefford RF. p14ARF interacts with the SUMO-conjugating enzyme Ubc9 and promotes the sumoylation of its binding partners. Cell cycle. 2005; 4:597–603. [PubMed: 15876874]
13. Tago K, Chiocca S, Sherr CJ. Sumoylation induced by the Arf tumor suppressor: a p53-independent function. PNAS. 2005; 102:7689–7694. [PubMed: 15897463]

14. Rocha S, Campbell KJ, Perkins ND. p53- and Mdm2-independent repression of NF-kB transactivation by the ARF tumor suppressor. Molecular cell. 2003; 12:15–25. [PubMed: 12887889]
15. Martin AC, Thornton JD, Liu J, Wang X, Zuo J, Jablonski MM, Chaum E, Zindy F, Skapek SX. Pathogenesis of persistent hyperplastic primary vitreous in mice lacking the arf tumor suppressor gene. Invest Ophthalmol Vis Sci. 2004; 45:3387–3396. [PubMed: 15452040]
16. McKeller RN, Fowler JL, Cunningham JJ, Warner N, Smeyne RJ, Zindy F, Skapek SX. The Arf tumor suppressor gene promotes hyaloid vascular regression during mouse eye development. Proc Natl Acad Sci USA. 2002; 99:3848–3853. [PubMed: 11891301]
17. Silva RL, Thornton JD, Martin AC, Rehg JE, Bertwistle D, Zindy F, Skapek SX. Arf-dependent regulation of Pdgf signaling in perivascular cells in the developing mouse eye. EMBO J. 2005; 24:2803–2814. [PubMed: 16037818]
18. Widau RC, Zheng Y, Sung CY, Zelivianskaia A, Roach LE, Bachmeyer KM, Abramova T, Desgardin A, et al. p19Arf represses platelet-derived growth factor receptor beta by transcriptional and posttranscriptional mechanisms. Molecular and cellular biology. 2012; 32:4270–4282. [PubMed: 22907756]
19. Freeman-Anderson NE, Zheng Y, Calla-Martin AC, Treanor LM, Zhao YD, Garfin PM, He TC, Mary MN, et al. Expression of the Arf tumor suppressor gene is controlled by Tgf{beta}2 during development. Development. 2009; 136:2081–2089. [PubMed: 19465598]
20. Gromley A, Churchman ML, Zindy F, Sherr CJ. Transient expression of the Arf tumor suppressor during male germ cell and eye development in Arf-Cre reporter mice. Proc Natl Acad Sci USA. 2009; 106:6285–6290. [PubMed: 19339492]
21. Zindy F, Williams RT, Baudino TA, Rehg JE, Skapek SX, Cleveland JL, Roussel MF, Sherr CJ. Arf tumor suppressor promoter monitors latent oncogenic signals in vivo. Proc Natl Acad Sci USA. 2003; 100:15930–15935. [PubMed: 14665695]
22. Langmead B, Salzberg SL. Fast gapped-read alignment with Bowtie 2. Nature methods. 2012; 9:357–359. [PubMed: 22388286]
23. Kim D, Salzberg SL. TopHat-Fusion: an algorithm for discovery of novel fusion transcripts. Genome biology. 2011; 12:R72. [PubMed: 21835007]
24. Trapnell C, Hendrickson DG, Sauvageau M, Goff L, Rinn JL, Pachter L. Differential analysis of gene regulation at transcript resolution with RNA-seq. Nature biotechnology. 2013; 31:46–53.
25. Zheng Y, Zhao YD, Gibbons M, Abramova T, Chu PY, Ash JD, Cunningham JM, Skapek SX. Tgfbeta signaling directly induces Arf promoter remodeling by a mechanism involving Smads 2/3 and p38 MAPK. J Biol Chem. 2010; 285:35654–35664. [PubMed: 20826783]
26. Kanehisa M, Goto S. KEGG: kyoto encyclopedia of genes and genomes. Nucleic acids research. 2000; 28:27–30. [PubMed: 10592173]
27. Kanehisa M, Goto S, Sato Y, Kawashima M, Furumichi M, Tanabe M. Data, information, knowledge and principle: back to metabolism in KEGG. Nucleic acids research. 2014; 42:D199–205. [PubMed: 24214961]
28. Zheng Y, Devitt C, Liu J, Iqbal N, Skapek SX. Arf induction by Tgfbeta is influenced by Sp1 and C/ebpbeta in opposing directions. PloS one. 2013; 8:e70371. [PubMed: 23940569]
29. Thornton JD, Swanson DJ, Mary MN, Pei D, Martin AC, Pounds S, Goldowitz D, Skapek SX. Persistent hyperplastic primary vitreous due to somatic mosaic deletion of the arf tumor suppressor. Invest Ophthalmol Vis Sci. 2007; 48:491–499. [PubMed: 17251441]
30. Suri C, Jones PF, Patan S, Bartunkova S, Maisonpierre PC, Davis S, Sato TN, Yancopoulos GD. Requisite role of angiopoietin-1, a ligand for the TIE2 receptor, during embryonic angiogenesis. Cell. 1996; 87:1171–1180. [PubMed: 8980224]
31. Armulik A, Genove G, Betsholtz C. Pericytes: developmental, physiological, and pathological perspectives, problems, and promises. Developmental cell. 2011; 21:193–215. [PubMed: 21839917]
32. Kalluri R, Zeisberg M. Fibroblasts in cancer. Nature reviews. Cancer. 2006; 6:392–401. [PubMed: 16572188]
33. Garlanda C, Dejana E. Heterogeneity of endothelial cells. Specific markers. Arteriosclerosis, thrombosis, and vascular biology. 1997; 17:1193–1202.

34. Byerly MS, Blackshaw S. Vertebrate retina and hypothalamus development. Wiley interdisciplinary reviews. Systems biology and medicine. 2009; 1:380–389. [PubMed: 20836003]

35. Subramanian A, Tamayo P, Mootha VK, Mukherjee S, Ebert BL, Gillette MA, Paulovich A, Pomeroy SL, et al. Gene set enrichment analysis: a knowledge-based approach for interpreting genome-wide expression profiles. Proceedings of the National Academy of Sciences of the United States of America. 2005; 102:15545–15550. [PubMed: 16199517]

36. Xu PX, Woo I, Her H, Beier DR, Maas RL. Mouse Eya homologues of the Drosophila eyes absent gene require Pax6 for expression in lens and nasal placode. Development. 1997; 124:219–231. [PubMed: 9006082]

37. Iqbal N, Mei J, Liu J, Skapek SX. miR-34a is essential for p19-driven cell cycle arrest. Cell cycle. 2014; 13

38. Dreszer TR, Karolchik D, Zweig AS, Hinrichs AS, Raney BJ, Kuhn RM, Meyer LR, Wong M, et al. The UCSC Genome Browser database: extensions and updates 2011. Nucleic acids research. 2012; 40:D918–923. [PubMed: 22086951]

39. Maragkakis M, Reczko M, Simossis VA, Alexiou P, Papadopoulos GL, Dalamagas T, Giannopoulos G, Goumas G, et al. DIANA-microT web server: elucidating microRNA functions through target prediction. Nucleic acids research. 2009; 37:W273–276. [PubMed: 19406924]

40. Morrison CD, Parvani JG, Schiemann WP. The relevance of the TGF-beta Paradox to EMT-MET programs. Cancer letters. 2013; 341:30–40. [PubMed: 23474494]

Method Summary

Here we describe the isolation of cells that express the *Arf* promoter from the primary vitreous space of the developing eye. Using mice in which exon 1β of the *Arf* gene is replaced with Gfp, we purified hyperplastic cells by FACS from the primary vitreous and expanded them in culture. These primary vitreous cells (PVCs) represent the first cell type in which the *Arf* gene product, $p19^{Arf}$, normally acts to block their aberrant accumulation *in vivo*, and this report is the first description of these cultured cells.

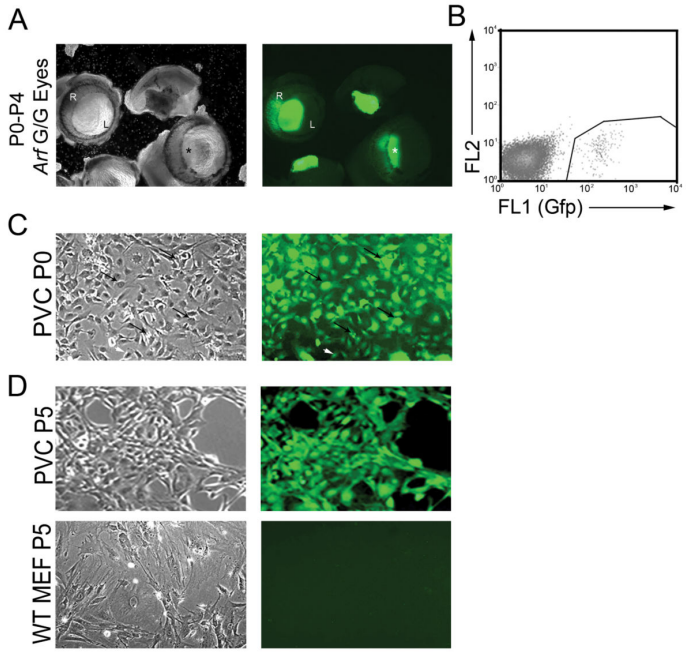

Figure 1. Isolation and expansion of $Arf^{GFP/GFP}$ PVCs

(A) Representative photomicrograph of enucleated mouse eyes from P0-P4 $Arf^{GFP/GFP}$ mice. Phase contrast image (left), GFP (right). The retrolental mass (*) is behind the lens (L) and expresses GFP. (R= retina) (B) Purification of PVCs by fluorescence activated cell sorting (FACS) for GFP. Representative images of cultured PVCs at passage 0 (C) and passage 5 (D). WT MEF (wild type mouse embryonic fibroblasts) cells at passage 5 (D). Phase contrast image (left), fluorescence image showing GFP expression (right). Arrows indicate heterogeneous GFP expression between high expressing (black) and low expressing (white) cells.

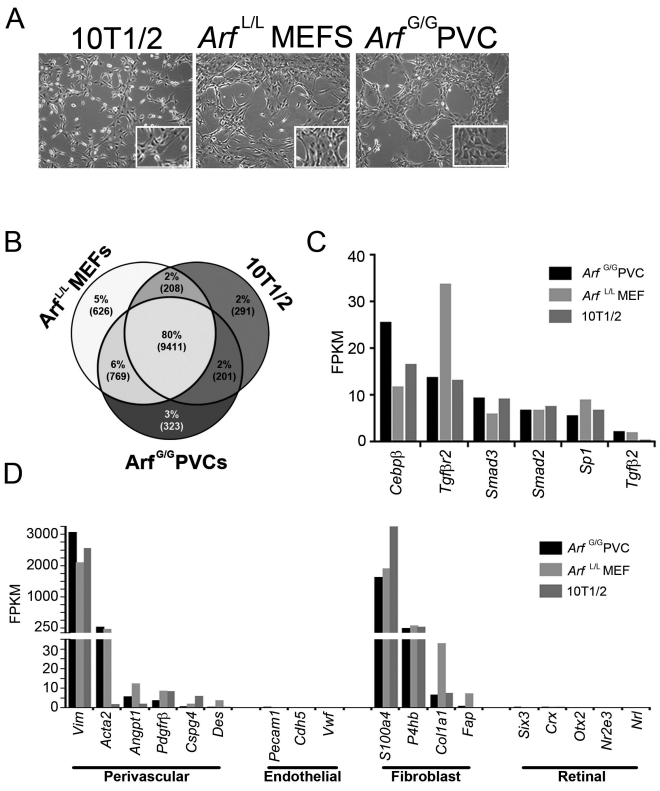

Figure 2. PVCs express perivascular genes

(A) Representative phase contrast image of 10T1/2, *Arf*$^{lacZ/lacZ}$ MEFs and *Arf*$^{GFP/GFP}$ PVCs in culture. (B) Venn diagram comparison of all genes expressed in the three cell lines showing unique and overlapping transcripts. (C) Expression of a subset of Tgf-beta pathway genes (FPKM) (D) Expression of cell type specific markers demonstrates that the PVCs express perivascular and fibroblast genes, not endothelial or retinal genes.

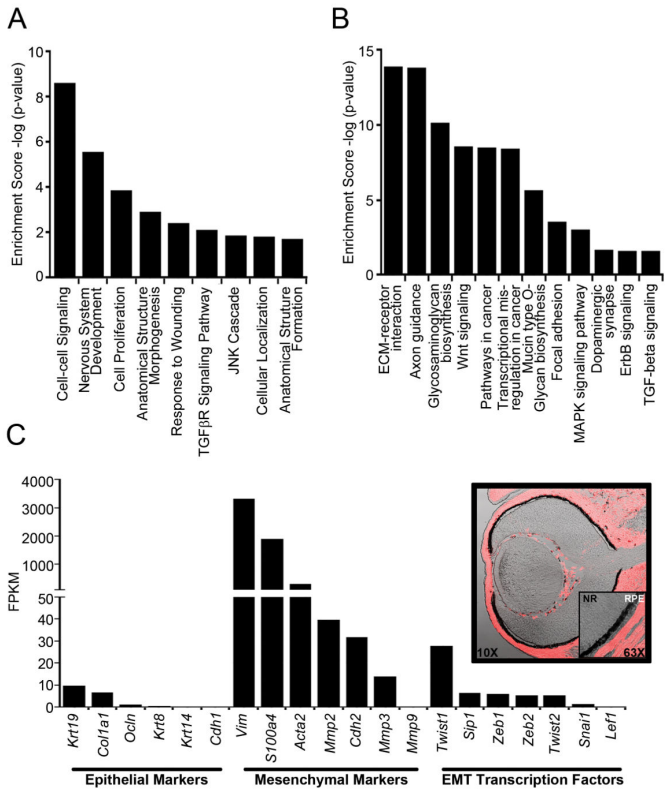

Figure 3. Gene set enrichment analysis of differentially expressed PVC genes identifies EMT related pathways

(A) Gene Ontology (GO) term enrichment analysis for the PVC only genes. Indicated are a subset of enriched pathways listed in order of significance (q>0.05). (B) KEGG Pathway analysis of microRNA target genes expressed in PVCs. microRNA target prediction was performed using Diana miRPath v2.0 Top ten pathways are listed in order of significance (q>0.05). (C) EMT marker gene expression in the PVCs (FPKM). Insert shows phase contrast and fluorescence overlay of Wnt1-cre, tdTomato e14.5 mouse eye. PVCs are derived from the neural crest (arrow) while retinal pigment epithelium (RPE) is not (arrowhead, inset).

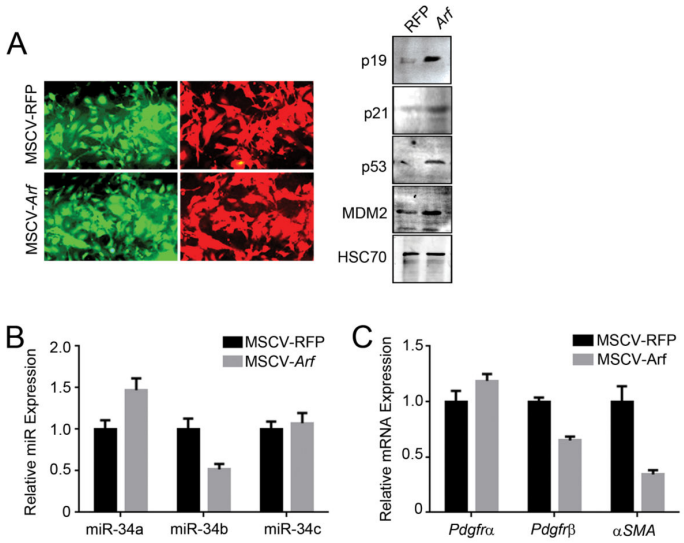

Figure 4. Ectopic p19^{Arf} expression in PVCs activates the p53 pathway

(A) Retroviral transduction of PVCs with MSCV-RFP (top panel) or MSCV-Arf (bottom panel). (B) Representative western blot showing induction of p21, p53 and MDM2 upon ectopic p19^{Arf} expression (C) Quantitative analysis by qRT-PCR of miR-34abc family in PVCs upon retroviral transduction of *Arf*. microRNA expression is normalized to U6 and represented as relative to RFP control (D) Quantitative analysis by qRT-PCR of Pdgfrα, Pdgfrβ and αSMA in PVCs transduced with RFP or Arf. Expression is relative to RFP control and normalized to Gapdh.